Velocity profile in a two-layer Kolmogorov-like flow

Balachandra Suri, Jeffrey Tithof, Radford Mitchell Jr., Roman O. Grigoriev, and Michael F. Schatz

Citation: Physics of Fluids (1994-present) **26**, 053601 (2014); doi: 10.1063/1.4873417
View online: http://dx.doi.org/10.1063/1.4873417
View Table of Contents: http://scitation.aip.org/content/aip/journal/pof2/26/5?ver=pdfcov
Published by the AIP Publishing

PHYSICS OF FLUIDS **26**, 053601 (2014)

Velocity profile in a two-layer Kolmogorov-like flow

Balachandra Suri, Jeffrey Tithof, Radford Mitchell, Jr., Roman O. Grigoriev, and Michael F. Schatz
Center for Nonlinear Science and School of Physics, Georgia Institute of Technology, Atlanta, Georgia 30332-0430, USA

(Received 24 July 2013; accepted 17 March 2014; published online 2 May 2014)

In this article, we discuss flows in shallow, stratified horizontal layers of two immiscible fluids. The top layer is an electrolyte which is electromagnetically driven and the bottom layer is a dielectric fluid. Using a quasi-two-dimensional approximation, which assumes a horizontal flow whose direction is independent of the vertical coordinate, we derive a generalized two-dimensional vorticity equation describing the evolution of the horizontal flow. Also, we derive an expression for the vertical profile of the horizontal velocity field. Measuring the horizontal velocity fields at the electrolyte-air and electrolyte-dielectric interfaces using particle image velocimetry, we validate the theoretical predictions of the horizontal velocity and its vertical profile for steady as well as for freely decaying Kolmogorov-like flows. Our analysis shows that by increasing the viscosity of the electrolyte relative to that of the dielectric, one may significantly improve the uniformity of the flow in the electrolyte, yielding excellent agreement between the analytical predictions and the experimental measurements. © *2014 AIP Publishing LLC*. [http://dx.doi.org/10.1063/1.4873417]

I. INTRODUCTION

The study of two-dimensional (2D) flows has received significant attention in recent decades with the aim of understanding turbulence.[1] Compared to their three-dimensional (3D) counterparts, 2D flows are more amenable to analytical and numerical analysis. However, fluid flows in practice are never strictly 2D, in the sense that the velocity field describing the flow depends on all three spatial coordinates and has non-zero components along all three spatial directions. However, flows in which the velocity along one of the spatial directions is greatly suppressed have been realized in a variety of systems which include flows in shallow electrolytic layers,[2] superfluid helium,[3] liquid metals,[4,5] soap films,[6] and electron plasmas.[7] The mechanism that leads to this suppression is different in each of these systems, demanding a specialized approach.

In this article, we discuss quasi-two-dimensional (Q2D) flows in shallow electrolytic layers. By quasi-two-dimensional, we mean flows which satisfy the following two conditions: (i) the components of velocity parallel to a plane (horizontal) are much stronger than the component perpendicular to it (vertical)[8] and (ii) the *direction* of the horizontal velocity does not depend on the vertical coordinate. Such flows have been studied extensively due to the simplicity of the experimental setup.

Fluid flows in shallow electrolytic layers have been realized experimentally in homogeneous[2] as well as stratified layers of fluids.[9,10] It was first observed by Bondarenko *et al.*,[2] for an experimental realization of the Kolmogorov flow (a planar unidirectional flow with a sinusoidal velocity profile)[11] in a homogeneous electrolytic layer, that the interaction of the flow with the solid boundary at the bottom resulted in dissipation that was not accounted for in the 2D Navier-Stokes equation (NSE). It was suggested that the addition of a linear term $(-\alpha\mathbf{u})$ to the 2D NSE modeled the dissipation satisfactorily;[2] this term is commonly referred to as the "Rayleigh friction" term. The stability of the laminar flow predicted by the 2D NSE with friction (NSE-WF) was in good agreement with the one experimentally observed. A more thorough discussion of related theoretical and experimental results is provided in the articles by Obukhov[12] and Thess.[13]

The questions of whether the experimental flows can be considered Q2D and whether the 2D NSE-WF is accurate attracted significant attention in the mid-1990s. Measuring the horizontal velocity field of a decaying dipolar vortex in an electrolyte layer, Paret *et al.*[14] inferred that the horizontal velocity, following a brief transient, relaxed to a Poiseuille-like profile in the vertical direction. The measured rate of decay was also in good agreement with that of plane Poiseuille flow.[15] However, there was no mention of the range of Reynolds numbers within which the experimental results agreed with those predicted by theory. Jüttner *et al.*[16] performed a direct numerical simulation (DNS) of the 2D NSE-WF, using experimental data to initialize the simulation, and showed that it did capture the evolution of the decaying flow, at least qualitatively. Later, Satijn *et al.*[17] analyzed the decay of a monopolar vortex using a full 3D DNS and reported a regime diagram showing that a weakly driven flow in shallow electrolytic layers (both homogeneous and stratified) remained Q2D during its decay. Following this study, Akkermans *et al.* performed experimental measurements of 3D velocity fields using Stereo Particle Image Velocimetry in a single layer setup[18,19] and a two-layer setup[20] at high Reynolds numbers ($Re \approx 2000$). Their results indicated that, at these Reynolds numbers, the vertical velocity component was comparable to the horizontal components and hence the flow could no longer be considered Q2D. To understand the transition of a Q2D flow to a 3D one, Kelley and Ouellette[21] performed experiments over a wide range of Reynolds numbers ($30 < Re < 250$) and showed that there is a critical Reynolds number ($Re_c \approx 200$), both for homogeneous and stratified layers, below which the flow can be considered Q2D. These studies, aimed at understanding the three-dimensionality of flows in shallow electrolytic layers, suggest that there are three mechanisms that lead to three-dimensionality. Ekman pumping,[19,21] which results from the variation of vorticity with depth, and interfacial deformations which drive gravity waves[20] are in play at all Reynolds numbers. Shear instability, on the other hand, sets in above a critical Reynolds number.[21]

Most experiments studying flows in shallow electrolytic layers were aimed at understanding 2D turbulence from a statistical perspective, requiring high Reynolds numbers to be realized.[9,14,22] However, in recent years, there has been moderate success, both on theoretical[23–26] and experimental fronts,[27,28] in understanding transitional and weak turbulence (both 2D and 3D) as dynamics guided by exact but unstable solutions (often referred to as exact coherent structures (ECS)) of the NSE. For instance, Chandler and Kerswell[29] have recently identified around 50 different ECS at low Reynolds numbers ($\mathrm{Re} \approx 40$) in a 2D DNS of turbulent Kolmogorov flow. This is a very significant result, since experimental flows at this Reynolds number can be considered Q2D.[17,21] However, aside from the study of Figueroa *et al.*,[30] to the best of our knowledge, there have been no attempts at making a quantitative comparison between experiments and numerical simulations of forced flows in shallow electrolytic layers. Hence, building a framework for a direct comparison between a Q2D flow and a 2D model used to describe such a flow is imperative. In particular, such a framework is necessary to describe how the flow is affected by the experimental parameters such as fluid layer depths, viscosity, density, and the forcing.

To compare the theoretical estimates from a 2D model with a Q2D experimental flow, we use an experimental realization of the Kolmogorov-like flow in a thin layer of electrolyte driven by a linear array of magnets with alternating polarity. Q2D flows driven by linear, as well as rectangular and triangular arrays of magnets, have been studied rigorously in the context of 2D turbulence.[13,31,32] The regularity of the laminar flow profiles in these systems allows considerable analytical and numerical progress, which makes them ideal for comparing with experiments. As opposed to the rectangular and triangular vortex arrays, the laminar Kolmogorov-like flow is essentially devoid of vortices and hence one can safely ignore the effects of both Ekman pumping and interfacial deformation, yielding a truly Q2D flow and enabling direct quantitative comparison between analytical solutions and experimental measurements at relatively low Reynolds numbers.

This article is organized as follows. In Sec. II, we derive a generalized 2D vorticity equation, describing the evolution of weakly driven flows in shallow electrolytic layers. We then present, in Sec. III, a brief description of our experimental realization of Kolmogorov flow in a stratified two-immiscible-layer configuration. In Sec. IV, we derive the equation for the vertical profile of the horizontal velocity field for two special flow configurations, the Kolmogorov-like flow and unidirectional flow. Using this profile, we evaluate analytical expressions for the coefficients that

appear in the vorticity equation. Using the Kolmogorov-like flow, in Sec. V, we validate the model by comparing theoretical predictions of the horizontal velocity with those measured experimentally. We discuss the effects of viscosity, magnetic field, and thickness of fluid layers on the coefficients that appear in the vorticity equation. Furthermore, we define a measure of two-dimensionality in the (forced) upper layer and show that it is possible to make the flow in that layer essentially 2D by increasing its viscosity relative to the (lubricating) lower layer. Section VI presents our conclusions and discusses the applications and the limitations of the 2D model.

II. GENERALIZED 2D VORTICITY EQUATION

Consider a shallow layer of fluid, with thickness h, in a laterally extended container with a flat bottom. By shallow, we mean that the characteristic horizontal length scale L is substantially larger than the thickness h. We assume the xy-plane is parallel to the bottom of the container and the z-axis is in the vertical direction, with $z = 0$ chosen at the bottom of the fluid layer and $z = h$ corresponding to the fluid-air interface (cf. Figure 1(b)). The velocity field in such flows is inherently three-dimensional, in the sense that it generally depends on all three coordinates, $\mathbf{V} = \mathbf{V}(x, y, z, t)$. This inherent three-dimensionality is due to the fact that the bottom of the fluid layer ($z = 0$) is constrained to be at rest due to the no-slip boundary condition. The velocity field in such a system is governed by the 3D Navier-Stokes equation for an incompressible fluid ($\nabla \cdot \mathbf{V} = 0$),

$$\rho(\partial_t \mathbf{V} + \mathbf{V} \cdot \nabla \mathbf{V}) = -\nabla p + \mu \nabla^2 \mathbf{V} + \mathbf{f} + \rho \mathbf{g}, \tag{1}$$

where ρ is the density of the fluid under consideration, μ is the dynamic viscosity, $\rho\mathbf{g}$ is the gravitational force (along the z-axis), and $\mathbf{f}$ is the electromagnetic force in the plane of the fluid (the xy-plane).

Equation (1), combined with the incompressibility condition, describes the evolution of the full 3D velocity field. However, for flows in shallow layers of fluid, driven by *weak, in-plane* forcing, the vertical velocity component is much smaller compared to the horizontal one.[17] In such flows the characteristic times describing equilibration of momentum in the vertical direction ($\rho h^2/\mu$) are much smaller than those associated with the horizontal directions ($\rho L^2/\mu$). This tends to align an unforced flow at a particular horizontal position (x, y) and different z along the same direction. Furthermore, if the *direction* of the forcing $\mathbf{f}$ is independent of z, this forcing will not destroy the alignment and we can assume the *direction* of the velocity to be independent of the height z allowing the velocity field to be factored as[30,33]

$$\mathbf{V}(x, y, z, t) = P(z)\mathbf{U}(x, y, t) \equiv P(z)[u_x(x, y, t)\hat{\mathbf{x}} + u_y(x, y, t)\hat{\mathbf{y}}], \tag{2}$$

where $P(z)$ describes the dependence of the horizontal velocity on z, and the unit vectors $\hat{\mathbf{x}}$ and $\hat{\mathbf{y}}$ lie in the horizontal plane. A thorough discussion on the validity of this Q2D approximation can found in Satijn *et al.*[17] The presence of the solid boundary at the bottom ($z = 0$) and of a free surface at the top ($z = h$) are accounted for by choosing $P(0) = 0$ and $P'(h) = 0$, where $P' = dP/dz$. Furthermore, we impose the normalization condition

$$P(h) = 1 \tag{3}$$

to make the factorization unique, so $\mathbf{U}(x, y, t)$ can be interpreted as the velocity of the free surface ($z = h$).

Substitution of (2) into (1) gives

$$\rho P \partial_t \mathbf{U} + \rho P^2 \mathbf{U} \cdot \nabla_\parallel \mathbf{U} = -\nabla_\parallel p + P\mu\nabla_\parallel^2 \mathbf{U} + \mathbf{U}\mu\nabla_\perp^2 P + \mathbf{f}, \tag{4}$$

$$\nabla_\perp p = \rho \mathbf{g},$$

along with $\nabla_\parallel \cdot \mathbf{U} = 0$, where the subscripts $\parallel$ and $\perp$ represent the horizontal and vertical components, respectively. In general, the profile $P(z)$ depends on the exact form of forcing $\mathbf{f}$ and the horizontal flow profile $\mathbf{U}$. However, we further assume that the profile $P(z)$ is independent of $\mathbf{U}$. This assumption, though not intuitive, proves to be valid at moderate Re, as we shall show for a couple of test cases below.

Integrating the first of the two equations in (4) over the z coordinate, i.e., from the bottom of the fluid layer ($z = 0$) to the free surface ($z = h$), and taking the curl, we obtain an equation for the vertical (z) component of the vorticity $\omega = \partial_x u_y - \partial_y u_x$,

$$\partial_t \omega + \beta \mathbf{U} \cdot \nabla_\parallel \omega = \bar{\nu} \nabla_\parallel^2 \omega - \alpha \omega + W. \tag{5}$$

The parameters β, $\bar{\nu}$, and α are defined as follows:

$$\beta = \frac{\int_0^h \rho P^2 dz}{\int_0^h \rho P dz}, \quad \bar{\nu} = \frac{\int_0^h \mu P dz}{\int_0^h \rho P dz}, \quad \alpha = \frac{(\mu P')_{z=0}}{\int_0^h \rho P dz}. \tag{6}$$

The source term W on the right-hand side of (5) corresponds to the z-component of the curl of the depth-averaged force density

$$W = \frac{\int_0^h (\partial_x f_y - \partial_y f_x) dz}{\int_0^h \rho P dz}. \tag{7}$$

In Eq. (5), the prefactor β to the advection term has been assumed equal to unity in all previous studies.[2,34] For a Poiseuille-like profile

$$P(z) = \sin\left(\frac{\pi z}{2h}\right), \tag{8}$$

which has traditionally been used to describe Q2D flows,[17] we have computed β using Eq. (6). It turns out that $\beta = \pi/4 \approx 0.79$ is significantly different from unity. The deviation of β from unity captures the decrease in the inertia of the fluid flow, since the velocity of the fluid closer to the solid boundary at the bottom is smaller than that near the free surface.

The parameter $\bar{\nu}$ is the depth-averaged kinematic viscosity. For a shallow, homogeneous layer of fluid, the depth-averaged kinematic viscosity ($\bar{\nu}$) is equal to the kinematic viscosity (ν) of the fluid. However, for stratified layers, fluid properties (μ, ρ) depend on z. In such a case, the integrals in Eqs. (6) and (7) are computed taking the variation in ρ and μ into account.

The linear friction term $-\alpha\omega$, which accounts for the presence of a solid boundary at the bottom of the fluid layer, is a direct consequence of ansatz (2) and depth-averaging. This is distinctly different from how previous studies have included this term in the 2D NSE-WF.[2,8] Using the Poiseuille-like profile (8), we can recover the expression $\alpha = \pi^2 \nu / 4h^2$ for the Rayleigh friction coefficient without assuming a decaying flow.[16,17]

Finally, in electromagnetically driven shallow electrolytic layers, the forcing $\mathbf{f}$ may depend on z, most commonly due to a decay in the magnetic field strength. The source term W takes the effect of such decay into account.

It is important to point out that the vorticity equation (5) is a 2D equation that *quantitatively* describes 3D flows in regimes where ansatz (2) is valid. In particular, ω describes the vorticity at the top surface of the electrolyte, facilitating direct comparison between experiment and analytical or numerical solutions.

III. EXPERIMENT

As mentioned earlier, Q2D flows in shallow layers of electrolytes have been realized experimentally in homogeneous as well as stratified electrolytic layers. The rationale behind using stratified layers is that the top layer—which is used for all the measurements—is shielded from the no-slip boundary condition at the bottom by a *lubricating* layer. Three stable configurations of stratified fluid layers have been employed for experimental realization of flows in shallow electrolyte layers. The first of these[22] used two *miscible* layers of saltwater having different densities, with the fluid in the bottom layer being heavier than the one in the top layer. In the second configuration, which is a variation of the one mentioned above, the electrolyte in the top layer was replaced by pure water.[21,35] The third stable configuration, suggested by Rivera and Ecke,[10] used a heavier, *immiscible* dielectric fluid as the lubricating bottom layer and a layer of electrolyte above it. Immiscibility complements stratification in suppressing vertical motion, thus enhancing two-dimensionality of the flow in

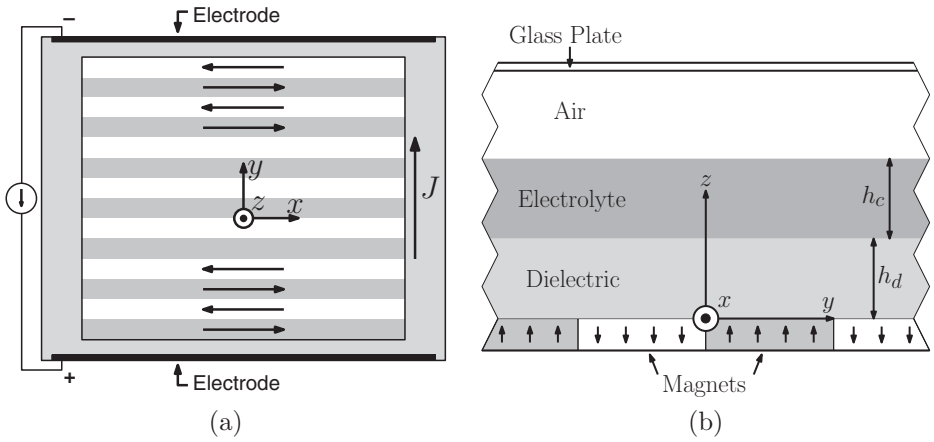

FIG. 1. The (a) top view and (b) transverse cross-section view of the experimental setup for quasi-2D Kolmogorov-like flow. The system contains two immiscible fluid layers: the bottom one is a dielectric fluid of thickness h_d and the top one is an electrolyte of thickness h_c. As a uniform, steady current with density J flows between the two electrodes through the electrolyte layer, a shear flow, represented by arrows in (a), is induced in the fluids by spatially alternating Lorentz forces. The arrows in (b) indicate the direction of magnetization.

the electrolyte. The two-immiscible-layer configuration also allows for achieving higher Reynolds numbers[10] compared with the miscible-layer setups. Numerical studies[17] comparing the vertical velocity components in these configurations have suggested that stratification and immiscibility indeed suppress 3D motion. Hence, we have chosen to use the two-immiscible-layer configuration to generate Q2D flows.

The setup, shown in Figure 1, consists of an array of magnets placed at the center of an acrylic box of dimensions 25.4 cm × 20.3 cm × 3.8 cm. A thin sheet (thickness ≈ 0.05 mm) of black contact paper is placed on top of the magnets to provide a uniform background for imaging. The top surface of the contact paper corresponds to the plane $z = 0$. The region $0 < z < h_d$ is filled with perfluorooctane, a dielectric fluid of viscosity $\mu_d = 1.30$ mPa s and density $\rho_d = 1769$ kg/m^3. Above this is a layer of a conducting fluid (electrolyte) of thickness h_c ($h_d < z < h_d + h_c$), which is completely immiscible with the dielectric fluid. For all experimental runs, the height of the dielectric fluid is chosen to be $h_d = 0.3 \pm 0.01$ cm. However, across different runs the thickness of the electrolyte layer is varied from $h_c = 0.2 \pm 0.01$ cm to $h_c = 0.4 \pm 0.01$ cm. For the electrolyte, we use either of the following: a "low-viscosity electrolyte" consisting of a 0.3 M solution of $CuSO_4$ (with viscosity $\mu_c = 1.12$ mPa s and density $\rho_c = 1045$ kg/m^3) or a "high-viscosity electrolyte" consisting of a 0.3 M solution of $CuSO_4$ with 50% glycerol by weight (with viscosity $\mu_c = 6.06$ mPa s and density $\rho_c = 1160$ kg/m^3). Immiscibility and density stratification maintain the relative configuration of the two layers. A small amount of surfactant (dish soap) is added to the electrolyte to decrease the surface tension, and a glass plate is placed on top of the box to limit evaporation. Two 24.1 cm × 0.3 cm × 0.6 cm copper electrodes fixed along the longitudinal boundaries on either side of the box are used to drive a steady current through the electrolyte. The Lorentz forces acting on the electrolyte set the fluid layers in motion.

To create a spatially periodic magnetic field, we construct a magnet array with 14 NdFeB magnets (Grade N42), each 15.2 cm long, 1.27 cm wide, and 0.32 cm thick (cf. Figure 1(a)). The magnetization is in the vertical (z) direction, with a surface field strength close to 0.3 T. The magnets are positioned side-by-side along their width to form a 15.2 cm × (14 × 1.27 cm) × 0.32 cm array such that adjacent magnets have fields pointing in opposite directions, along the z-axis. The resulting net magnetic field $\mathbf{B}(y, z)$, close to the surface of the magnets, is quite complicated. However, experimental measurements (using a F. W. Bell Model 6010 Gaussmeter) show that the profile for the z-component of the magnetic field, B_z, is approximately sinusoidal in y beyond a height of $z = 0.25$ cm (the measurements for the center pair of magnets are shown in Figure 2(a)). The spatial period of the magnetic field sets the horizontal length scale $L = 1.27$ cm equal to the width of one

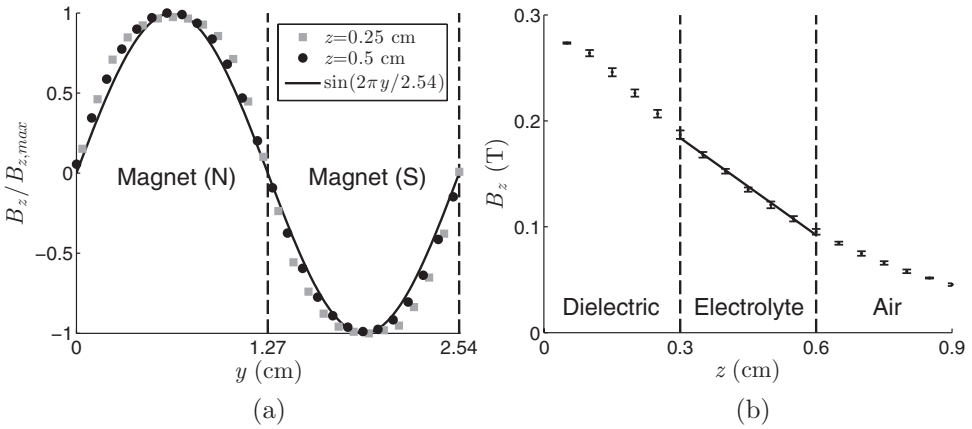

FIG. 2. (a) Experimental measurements of the transverse variation of the z-component of the magnetic field, B_z, above the middle two magnets of the magnet array, normalized by the maximum value of B_z for fixed z, $B_{z,\,max}$. A sine wave with periodicity equal to the width of one magnet pair is shown for comparison. (b) Experimental measurements of the decay of B_z with increasing height (z) from the magnets' surface. Error bars indicate one standard deviation.

magnet. Furthermore, we find B_z above the magnets to decay approximately linearly with z within the typical position of the electrolyte layer (0.3 cm $\leq z \leq$ 0.6 cm) (see Figure 2(b)). The parameters we find for the fit $B_z = B_1 z + B_0$ (at the maximum in y) are $B_1 = -30.6 \pm 0.5$ T/m and $B_0 = 0.276 \pm 0.01$ T.

In the electrolyte-dielectric setup described above, using tracer particles of different densities, one can visualize the flow either at the electrolyte-dielectric interface or at the free surface.[14] To visualize the flow at the free surface we use Glass Bubbles (K15) manufactured by 3M, sieved to obtain particles with mean radius $r = 24.5 \pm 2$ μm and mean density $\rho \approx 150$ kg/m^3. For seeding the interface, we use Soda Lime Solid Glass Microspheres manufactured by Cospheric with mean radius $r = 38 \pm 4$ μm and mean density $\rho = 2520$ kg/m^3. The soda lime microspheres, though denser than the dielectric fluid, stay trapped between the dielectric and electrolyte layers due to interfacial tension. The top surface of the electrolyte and the interface are not seeded simultaneously, but in separate experimental realizations. We use blue light-emitting diodes to illuminate the tracer particles.

The images of the flow are recorded using a Unibrain Fire-i Board B/W digital camera which has a CCD sensor with a resolution of 640 × 480 pixels. The flow field captured corresponds to a region at the center of the magnet array with dimensions 4.7 cm × 3.5 cm. Images are captured at equal intervals of 0.133 s, which corresponds to a frame rate of 7.5 Hz. Particle Image Velocimetry (PIV) was performed on the recorded images using Open Source Image Velocimetry software package (version 2.1, available at http://osiv.sourceforge.net/).

As mentioned earlier, the flow is driven by Lorenz forces resulting from the interaction between the magnetic field and a direct current passing through the electrolyte layer. In the experiments using the low-viscosity electrolyte, where the thickness of the electrolyte layer is varied from 0.2 cm to 0.4 cm, a direct current of 2.1 mA is passed through the electrolyte. Increasing the thickness of the electrolyte layer, keeping the total current constant, corresponds to decreasing the current density from $J = 4.26$ A/m^2 to $J = 2.13$ A/m^2. Similarly, in the experiments using the high-viscosity electrolyte, a direct current of 5.0 mA is passed through the electrolyte. The current density, for electrolyte thickness between 0.2 cm and 0.4 cm, ranges from $J = 10.16$ A/m^2 to $J = 5.08$ A/m^2.

We conclude this section by defining the Reynolds number characterizing the Q2D flows discussed in this article. Since $\mathbf{U}(x, y, t)$ (cf. Eq. (2)) is the horizontal velocity field at the free surface ($z = h_d + h_c$), which directly corresponds to our experimentally measurements, we define the velocity scale characterizing the flow as $U = \sqrt{\langle \mathbf{U} \cdot \mathbf{U} \rangle} = \sqrt{\langle u_x^2 + u_y^2 \rangle}$, where $\langle \dots \rangle$ denotes the spatial average. The Reynolds number is then defined as $Re = UL/\bar{\nu}$. This is similar to the

definition used in the article by Kelley and Ouellette[21] discussing the onset of three-dimensionality, thus facilitating a straightforward inference regarding when the flow starts to deviate from being Q2D.

IV. VELOCITY PROFILE IN THE TWO-IMMISCIBLE-LAYER SETUP

In this section, we solve for the vertical profile $P(z)$ of the horizontal velocity (cf. Eq. (2)) in two special cases, a Kolmogorov-like flow and a unidirectional flow. The case of the Kolmogorov-like flow allows direct comparison of theoretical predictions with experimental measurements. The unidirectional flow cannot be realized in experiment, but allows derivation of simple expressions for α, $\bar{\nu}$, and β in the generalized 2D vorticity equation (5), which are helpful in understanding the parametric dependence of these coefficients.

A. Kolmogorov-like flow

To solve for the velocity profile $P(z)$ in (2) within the two immiscible layers described in the experiment, we assume that the magnet array is infinitely long in the x (longitudinal) direction and periodic in the y (transverse) direction. By symmetry, the array of magnets produces a field that has no component along the longitudinal direction:

$$\mathbf{B} = B_y(y, z)\hat{\mathbf{y}} + B_z(y, z)\hat{\mathbf{z}}. \tag{9}$$

Within the electrolyte, the z-component of the magnetic field can be modeled to vary linearly with z and sinusoidally with y (cf. Figure 2). Hence we can write

$$B_z = (B_1 z + B_0)\sin(\kappa y), \tag{10}$$

where $\kappa = \pi/L$. A uniform and constant current with density $\mathbf{J} = J\hat{\mathbf{y}}$ passing through the electrolyte along the transverse direction results in a Lorentz force density along the $\hat{\mathbf{x}}$ direction which is given by

$$\mathbf{f} = \mathbf{J} \times \mathbf{B} = \begin{cases} J(B_1 z + B_0)\sin(\kappa y)\hat{\mathbf{x}}, & h_d < z < h_d + h_c, \\ 0, & 0 < z < h_d \end{cases} \tag{11}$$

in the electrolyte and the dielectric, respectively.

For a current density (J) smaller than some critical value, the direction of the horizontal flow profile $\mathbf{U}$(x, y, t) follows that of the forcing (11), so we can look for laminar solutions of the form

$$\mathbf{U}(x, y, t) = u_0 \sin(\kappa y)\hat{\mathbf{x}}. \tag{12}$$

Substituting this into (4) yields a hydrostatic pressure distribution and a boundary value problem for the vertical profile $P(z)$,

$$\begin{aligned} P'' - \kappa^2 P &= -\frac{J}{u_0 \mu_c}(B_1 z + B_0), \quad h_d < z < h_d + h_c, \\ P'' - \kappa^2 P &= 0, \qquad\qquad\qquad\quad 0 < z < h_d, \end{aligned} \tag{13}$$

where the prime denotes differentiation with respect to z.

The boundary conditions that $P(z)$ must satisfy are the no-slip boundary condition at the bottom of the dielectric ($z = 0$), the continuity of the velocity and stress at the dielectric-electrolyte interface ($z = h_d$), and the stress-free boundary condition at the top (free) surface of the electrolyte ($z = h_d + h_c$),

$$P(0) = 0, \quad P(h_d^-) = P(h_d^+), \quad \mu_d P'(h_d^-) = \mu_c P'(h_d^+), \quad P'(h_d + h_c) = 0. \tag{14}$$

The solution to the differential equations (13) is given by

$$P_\kappa = \begin{cases} Ce^{\kappa z} + De^{-\kappa z} + \frac{JB_1}{u_0\mu_c\kappa^2}z + \frac{JB_0}{u_0\mu_c\kappa^2}, & h_d < z < h_d + h_c, \\ Ee^{\kappa z} + Fe^{-\kappa z}, & 0 < z < h_d. \end{cases} \tag{15}$$

In Eq. (15), in addition to the coefficients C, D, E, and F, the amplitude u_0 of the sinusoidal velocity profile at the free surface of the electrolyte is not known *a priori*. To uniquely define $P_\kappa(z)$ we also require the normalization condition $P_\kappa(h_c + h_d) = 1$, which is the analog of Eq. (3). This gives us the fifth equation, in addition to the four defined by Eq. (14), necessary to solve for the five unknowns C, D, E, F, and u_0.

As stated earlier, the motivation behind using stratified layers of fluids to realize Q2D flows is that the top layer is shielded from the no-slip boundary condition at the bottom by a lubricating layer. For a perfectly two-dimensional flow, one would expect the velocity field in the top layer to be independent of the z coordinate. Hence, for the two-immiscible-layer setup we can use the ratio of velocity at the free surface to that at the electrolyte-dielectric interface as a measure that characterizes the inherent deviation from two-dimensionality

$$s = \frac{P(h_d + h_c)}{P(h_d)}. \tag{16}$$

For a monotonically varying profile, the value of s describes how strongly the magnitude of the horizontal velocity field varies with z in the electrolyte, with $s = 1$ corresponding to a z-independent velocity profile. This measure of deviation from two-dimensionality is different from the one used in previous studies,[17,18] where the ratio of kinetic energy contained in the secondary flow to that in the primary (horizontal) flow was chosen as a measure of three-dimensionality. The functional form of expression (16) for the Kolmogorov-like flow is quite unwieldy and does not allow one to easily deduce the dependence on experimental parameters. Furthermore, closed form expressions for the coefficients (6) in the generalized 2D vorticity equation also turn out to be too complicated to yield much insight.

B. Unidirectional flow

We can derive a relatively simple analytical expression for the ratio of velocities in the special case where we ignore the y-dependence of the magnetic field B_z, i.e., $B_z = B_1 z + B_0$. The laminar flow is then unidirectional, i.e., $\mathbf{U}(x, y, t) = u_0\hat{\mathbf{x}}$. This flow can be interpreted as a limiting case of the Kolmogorov-like flow when the magnets are very wide ($\kappa \to 0$), and one confines observation to a small region near the centers of the magnets ($\kappa y \to n\pi/2$). The solution (15) is then replaced by

$$P_0 = \begin{cases} -\frac{JB_1}{6u_0\mu_c}z^3 - \frac{JB_0}{2u_0\mu_c}z^2 + Cz + D, & h_d < z < h_d + h_c, \\ Ez + F, & 0 < z < h_d. \end{cases} \tag{17}$$

We have calculated the unknown coefficients C, D, E, F, and u_0 in the above equation using the boundary conditions (14) and have included analytical expressions in the Appendix. Although the functional forms (15) and (17) of the velocity profile are quite different for the Kolmogorov flow and the unidirectional flow, their shape is virtually indistinguishable, as Figure 3 illustrates. This suggests that Q2D flows with arbitrary horizontal flow profiles $\mathbf{U}(x, y, t)$ and moderately high Reynolds numbers (up to $Re \approx 40$) may be accurately described using the simple velocity profile (17).

Using $P_0(z)$ we now calculate an analytical expression for the ratio (s) of the velocity at the free surface to that at the electrolyte-dielectric interface

$$s = 1 + \frac{1}{2}\frac{\mu_d h_c}{\mu_c h_d}\left(1 + \frac{1}{6}\frac{\Delta B}{\langle B\rangle}\right), \tag{18}$$

where $\Delta B = B_1 h_c$ is the change in magnetic field across the electrolyte and $\langle B\rangle = B_0 + B_1 h_d + \frac{1}{2}B_1 h_c$ is the mean magnetic field in the electrolyte.

The coefficients (6) that appear in the generalized 2D vorticity equation (5), in addition to depending explicitly on the experimental parameters, depend on the profile $P(z)$ as well. Since the

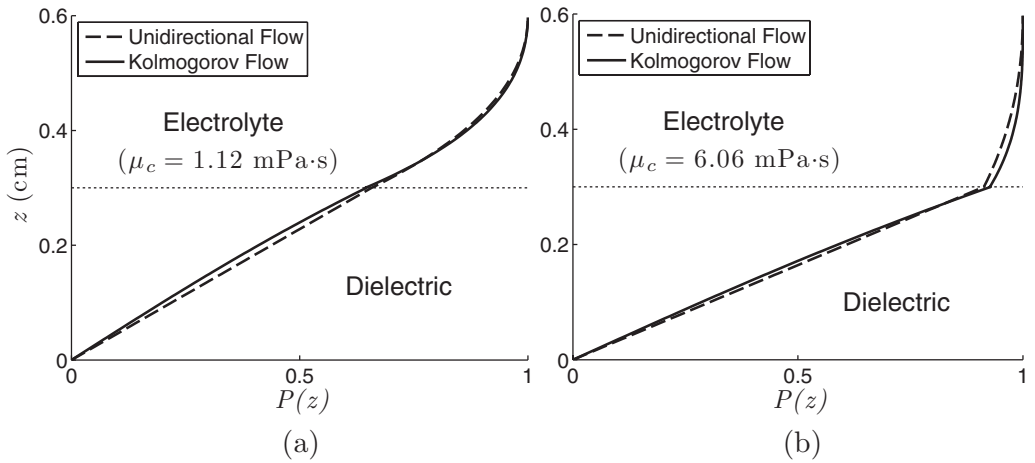

FIG. 3. Analytical results for the vertical profile of the horizontal flow field in both layers, with $h_d = h_c = 0.3$ cm, for (a) the low-viscosity electrolyte and (b) the high-viscosity electrolyte. The ratios of the velocities, as defined by (16), are: (a) uniform flow: $s_{low} = 1.52$, Kolmogorov flow: $s_{low} = 1.54$, and (b) uniform flow: $s_{high} = 1.10$, Kolmogorov flow: $s_{high} = 1.08$.

shapes of the profiles $P_0(z)$ and $P_\kappa(z)$ are virtually indistinguishable, we can evaluate analytical expressions for the coefficients (6) using $P_0(z)$. For the Rayleigh friction coefficient, using the velocity profile $P_0(z)$ we obtain

$$\alpha = \frac{\frac{\mu_d}{\rho_c}\frac{1}{h_d h_c}}{1 + \frac{1}{2}\frac{h_d}{h_c}\frac{\rho_d}{\rho_c} + \frac{1}{3}\frac{h_c}{h_d}\frac{\mu_d}{\mu_c}\left(1 + \frac{1}{8}\frac{\Delta B}{\langle B\rangle}\right)}. \tag{19}$$

For the depth-averaged kinematic viscosity, we obtain

$$\bar{\nu} = \nu_c \frac{1 + \frac{1}{2}\frac{h_d}{h_c}\frac{\mu_d}{\mu_c} + \frac{1}{3}\frac{h_c}{h_d}\frac{\mu_d}{\mu_c}\left(1 + \frac{1}{8}\frac{\Delta B}{\langle B\rangle}\right)}{1 + \frac{1}{2}\frac{h_d}{h_c}\frac{\rho_d}{\rho_c} + \frac{1}{3}\frac{h_c}{h_d}\frac{\mu_d}{\mu_c}\left(1 + \frac{1}{8}\frac{\Delta B}{\langle B\rangle}\right)}. \tag{20}$$

The exact expression for β is too complicated to yield much insight, but it can be evaluated using the profile $P_0(z)$ and the coefficients listed in the Appendix for any set of experimental parameters. It should be noted that, for the values of parameters used in the experiment, the coefficients s, α, $\bar{\nu}$, and β have a very weak dependence on $\epsilon = \Delta B/\langle B\rangle$: setting $\epsilon = 0$ changes the values by less than 5%. In the limit where the $\epsilon = 0$, we find

$$\beta = \frac{1 + \frac{1}{3}\frac{h_d}{h_c}\frac{\rho_d}{\rho_c} + \frac{2}{3}\frac{h_c}{h_d}\frac{\mu_d}{\mu_c} + \frac{2}{15}\frac{h_c^2}{h_d^2}\frac{\mu_d^2}{\mu_c^2}}{1 + \frac{1}{2}\frac{h_d}{h_c}\frac{\rho_d}{\rho_c} + \frac{5}{6}\frac{h_c}{h_d}\frac{\mu_d}{\mu_c} + \frac{1}{4}\frac{\rho_d}{\rho_c}\frac{\mu_d}{\mu_c} + \frac{1}{6}\frac{h_c^2}{h_d^2}\frac{\mu_d^2}{\mu_c^2}}. \tag{21}$$

Similarly, the dependence on κ is also very weak: evaluating the coefficients using $P_\kappa(z)$ instead of $P_0(z)$ changes their values by less than 6% (for the high-viscosity electrolyte).

V. RESULTS

A. Enhanced two-dimensionality in the electrolyte

Expression (18) suggests that even if the magnetic field across the electrolyte were uniform, i.e., $\Delta B = 0$, the flow in the electrolyte would still deviate significantly from being perfectly 2D. For a typical case where $\mu_c = \mu_d$ and $h_c = h_d$, one obtains $s = 1.5$. Using instead the value $\epsilon = -0.6$ corresponding to the experiment gives $s = 1.45$. Hence, the decay in the magnetic field does *not* contribute significantly to the deviation from two-dimensionality. Expression (18) also suggests that the shallower the electrolyte layer is (relative to the dielectric layer), the closer one comes to a

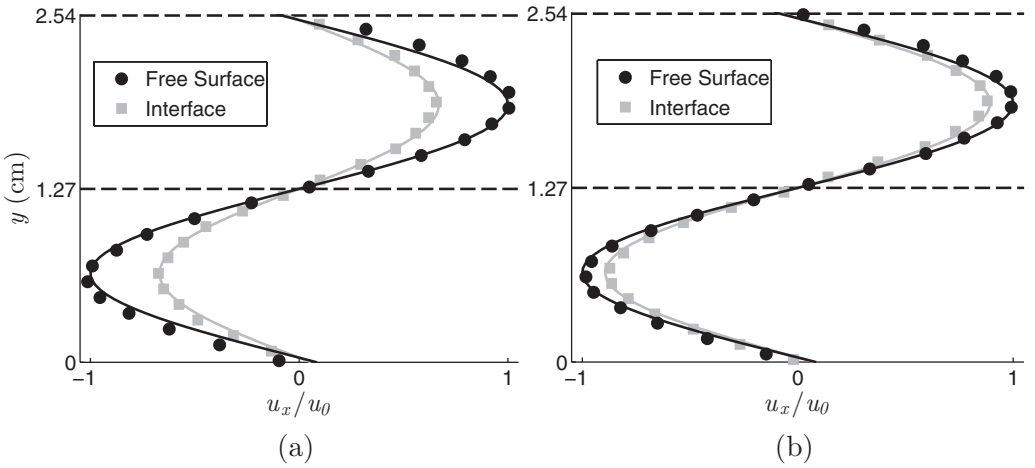

FIG. 4. Experimental measurements of the horizontal flow profile in the electrolyte layer, with $h_d = h_c = 0.3$ cm, taken separately at the free surface (black circles) and at the electrolyte-dielectric interface (gray squares). The plots correspond to (a) the low-viscosity electrolyte and (b) the high-viscosity electrolyte. PIV measurements are plotted for the time-independent laminar flow near the center of the magnet array; each data point is time-averaged over 5 min and spatially averaged over 4.5 cm along the x-direction to obtain an accurate estimate of the mean. A sine wave with fixed periodicity is fit to each data set, and the velocities are normalized by the amplitude of the top layer fit, u_0. Error bars are smaller than the size of the symbols.

vertically uniform profile in the electrolyte ($s = 1$). However, electrolyte layers with thickness less than 0.25 cm are found to be unstable in the experiment, as they break open to form configurations that correspond to lower total surface energy. Alternatively, one may increase the thickness h_d of the dielectric layer. This has the drawback that one moves farther from the magnets, requiring larger currents to drive the flow. Also, the Q2D approximation, an assumption whose validity depends partially on strong geometric confinement, is compromised. Hence, the most straightforward way to make the flow in the electrolyte nearly two-dimensional is by increasing the ratio of viscosities. The optimal choice of the electrolyte viscosity is not obvious. For the variation in the velocity of the electrolyte to be at most 10%, μ_c should exceed the solution of (18) with $s = 1.1$. Substituting the typical values of $\mu_d = 1.30$ mPa s, $\epsilon = -0.6$ and $h_d = h_c$ gives $\mu_c \geq 5.85$ mPa s. Indeed, comparison of the analytical velocity profiles presented in Figure 3 shows that the uniformity of the velocity in the conducting layer should be substantially enhanced when a more viscous electrolyte (with $\mu_c = 6.06$ mPa s) is used. This is experimentally validated by comparing the measured horizontal velocity of the laminar flow at the top and bottom surfaces of the electrolyte layer. As Figure 4 shows, the flow in the high-viscosity electrolyte is much closer to being vertically uniform ($s_{\text{high}} = 1.08$) than in the low-viscosity electrolyte ($s_{\text{low}} = 1.54$).

A higher viscosity means a higher current is necessary to reach a desirable Reynolds number; a potential drawback of this is the possibility of excess Joule heating, which can cause significant variation in the viscosity. However, 60 minute-long experiments using the high-viscosity electrolyte, where a steady current forces a flow with $Re \approx 40$, have shown that the fluid temperature increases only by around 1 °C. Hence in the regime of interest the effects of Joule heating are rather small.

B. Comparison between theory and experiment

Figure 5 shows experimental measurements of the velocity amplitude of the laminar flow at the free surface and the electrolyte-dielectric interface as the thickness h_c of the electrolyte layer is varied, while keeping the current I constant. For the experimental runs using the low-viscosity electrolyte (cf. Figure 5(a)) the Reynolds number of the flow decreases from $Re = 26.6$ to $Re = 17.1$ as the thickness of the electrolyte layer is increased from 0.2 cm to 0.4 cm. Similarly, for those using the high-viscosity electrolyte (cf. Figure 5(b)) the Reynolds number decreases from $Re = 7.9$ to $Re = 3.1$. Also plotted for comparison are the theoretical predictions of $u_0 P_\kappa(h_d + h_c) = u_0$ and $u_0 P_\kappa(h_d)$

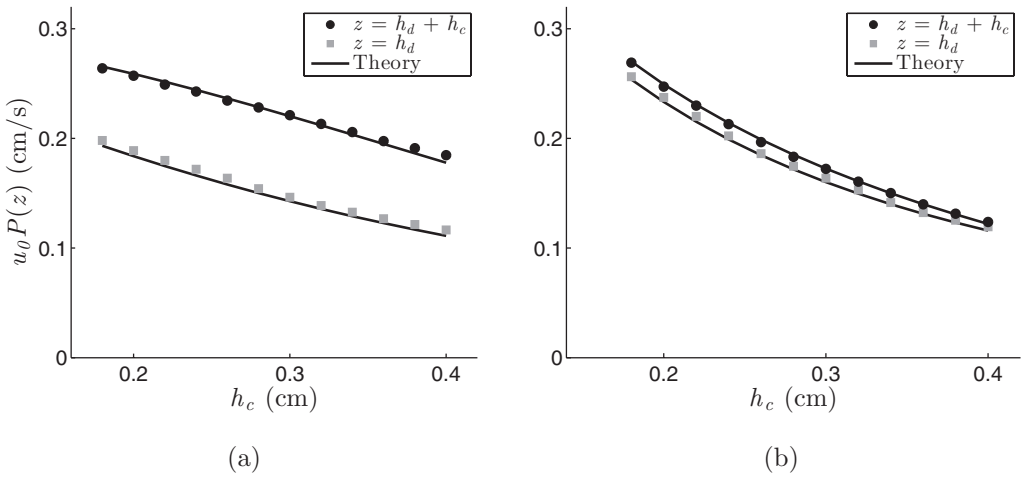

FIG. 5. Comparison of experimental and theoretical results for $u_0 P_\kappa(h_c + h_d)$ and $u_0 P_\kappa(h_d)$, which correspond to the amplitude of the sinusoidal velocity profile at the free surface and the electrolyte-dielectric interface, respectively. Here, h_c is varied while $h_d = 0.3$ cm is held constant. Plots correspond to (a) the low-viscosity electrolyte (with constant current $I = 2.1$ mA) and (b) the high-viscosity electrolyte (with constant current $I = 5.0$ mA). PIV measurements of the time-independent laminar flow are time-averaged over 5 min to reduce experimental noise and then fit with a sine wave with fixed periodicity. Error bars are smaller than the size of the symbols.

$= u_0/s$, which denote the velocity amplitude at the free surface and that at the electrolyte-dielectric interface, respectively. Most importantly, all the parameters used in the theoretical calculations have been measured experimentally. As can be seen from the plots, the relative difference between theory and experiment, for electrolytes of both viscosities, is less than 5%.

C. Coefficients in the generalized 2D vorticity equation

The motivation behind estimating the shape of the profile $P(z)$ in the two-immiscible-layer setup was, in part, to determine the coefficients (6) that appear in the generalized 2D vorticity equation (5). For $h_c = h_d = 0.3$ cm, using the low-viscosity electrolyte ($\mu_c = 1.12$ mPa s), we obtain $\beta = 0.73$, $\bar{\nu} = 0.94 \times 10^{-6}$ m^2 s^{-1}, and $\alpha = 0.063$ s^{-1}. This estimate of the Rayleigh friction coefficient is a factor of two smaller than the one suggested by Rivera and Ecke.[10] For the high-viscosity electrolyte ($\mu_c = 6.06$ mPa s), we obtain $\beta = 0.82$, $\bar{\nu} = 3.35 \times 10^{-6}$ m^2 s^{-1}, and $\alpha = 0.068$ s^{-1}. It is important to note that the Rayleigh friction coefficient remains fairly insensitive to the viscosity of the electrolyte. This has a significant consequence that one can change the relative importance of the diffusion term ($\bar{\nu}\nabla_\parallel^2\omega$) and the friction term ($-\alpha\omega$) in the vorticity equation (5) by changing the viscosity of the upper layer in the experiment. Interestingly, the Rayleigh friction coefficient for the two-immiscible-layer system is *not* very different from the one computed for a homogeneous layer of fluid. Using a Poiseuille-like vertical profile (8) and choosing $h = h_c + h_d = 0.6$ cm and $\bar{\nu} \approx 1 \times 10^{-6}$ m^2 s^{-1} we obtain $\alpha = \pi^2\bar{\nu}/4h^2 \approx 0.07$ s^{-1}.

D. Spin-down comparison

After the forcing is switched off, $W = 0$, the flow decays to rest exponentially fast, dissipating energy via bottom friction ($-\alpha\omega$) as well as horizontal diffusion of vorticity ($\bar{\nu}\nabla_\parallel^2\omega$). The solution of (5) corresponding to the initial condition (12) describing Kolmogorov flow and $W = 0$ is $\omega(x, y, t) = \omega_0 \exp(-t/\tau)\cos(\kappa y)$, where the decay rate is given by

$$\tau^{-1} = \alpha + \kappa^2\bar{\nu}. \tag{22}$$

As a check of the 2D model, we compare this prediction with the temporal evolution of the flow in experiment by letting it decay to rest from the steady laminar state by turning the forcing off.

After a brief transient, the velocity profile $\mathbf{U}(x, y, t) = u_0(t)\sin(\kappa y)$ measured at the free surface of the electrolyte decays exponentially, $u_0(t) \sim \exp(-t/\tau)$. These measurements yield a decay rate of $\tau_{\text{low}}^{-1} = 0.14 \pm 0.01\ \text{s}^{-1}$ for the low-viscosity electrolyte and $\tau_{\text{high}}^{-1} = 0.3 \pm 0.01\ \text{s}^{-1}$ for the high-viscosity one. In comparison, the analytical solution (22) yields $\tau_{\text{low}}^{-1} = 0.12 \pm 0.007\ \text{s}^{-1}$ for the low-viscosity electrolyte and $\tau_{\text{high}}^{-1} = 0.29 \pm 0.009\ \text{s}^{-1}$ for the high-viscosity one. It is important to note that Eq. (22) does not account for the change in the shape of the profile $P_\kappa(z)$ during the decay, which likely explains the slight disagreement between the theory and experiment at low μ_c. This indicates that the effect of relaxation of the profile, when the forcing is turned off, is more significant when using the low-viscosity electrolyte than when using the high-viscosity one, indicating that the profile in the higher viscosity electrolyte *may* be robust to time dependence. This is a non-trivial result: although the flow in the high-viscosity electrolyte is very nearly two-dimensional, the flow in the dielectric never is.

E. Measured normalized in-plane divergence

Experimentally realized Kolmogorov-like flow exhibits temporally complicated (aperiodic) dynamics above $Re \approx 30$. To verify the validity of the Q2D approximation (2) in this regime, up to $Re \approx 50$, we have computed the normalized in-plane divergence

$$\Lambda = \frac{h_c \iint |\nabla_\parallel \cdot \mathbf{U}| dx dy}{L \iint |\omega| dx dy}, \tag{23}$$

of the horizontal velocity field, experimentally measured at the free surface ($z = h_d + h_c$). This measure, used by Akkermans *et al.*,[20] characterizes the ratio of the horizontal velocity to the vertical velocity. For both the low- and high-viscosity electrolyte of typical thickness $h_c = 0.3$ cm, Λ varies from about 0.01 to 0.02, with no clear systematic trend. Since small errors in measuring velocities can contribute significantly to the value of the divergence computed, it is safe to say that $\Lambda = 0.02$ provides an upper bound for the relative strength of the secondary flow for $Re \leq 50$. This is approximately an order of magnitude smaller than values reported for numerical simulations in the range $1150 < Re < 2000$ for the dipolar vortex studied by Akkermans *et al.*[20] This indicates that for our system, even in the regime with temporally complicated dynamics, the deviation from a Q2D flow is small.

VI. CONCLUSION

Moderate Reynolds number flows in thin fluid layers supported by a solid surface have long been modeled by semi-empiric generalizations of the 2D Navier-Stokes equation. In this article, starting from the 3D Navier-Stokes equation and assuming the flow to be quasi-two-dimensional, i.e., having only horizontal components of velocity whose direction is independent of the vertical coordinate, we derive the proper 2D evolution equation for flows in homogeneous as well as stratified layers of fluid. The Rayleigh friction term in this generalized 2D vorticity equation, which models the presence of the no-slip boundary condition at the bottom of the fluid layer, appears naturally as a consequence of depth-averaging the 3D Navier-Stokes equation. Furthermore, we have shown that the advection term acquires a numerical prefactor which is different from unity. The evolution equation has been validated by testing it for self-consistency using different analytic solutions for steady flows and also by comparing its predictions with experiment for steady and freely-decaying Kolmogorov-like flows.

In addition to deriving the generalized vorticity equation, we have addressed the issue of inherent three-dimensionality of the two-layer flows, quantifying it in terms of the ratio of the fluid velocity at the top and bottom surface of the upper (driven) layer. Using this measure, we have shown that increasing the viscosity of the fluid in the upper layer with respect to the viscosity of the bottom (lubricating) layer makes the flow in the upper layer much closer to being uniform (2D), which is advantageous because (i) the agreement between the predictions of the 2D model for both steady and freely decaying laminar flows improves considerably, suggesting that the model *may* remain quantitatively accurate for other time-dependent flows, and (ii) the gradient of the horizontal velocity

along the vertical direction is greatly reduced, which in turn results in a significant suppression in the Ekman pumping.

Recent studies[29] aimed at understanding 2D turbulence from a dynamical systems perspective have found an abundance of ECS of the 2D NSE with periodic boundary conditions at $Re \approx 40$. The 2D NSE, however, does not govern the evolution of Q2D flows. Our experiments, as well as those of other groups,[21] show that at $Re \approx 40$ flows in shallow electrolytic layers are Q2D. Hence to compute the ECS that are expected to organize the weakly turbulent experimental flows, one has to use the 2D generalized vorticity equation (5). Whether this 2D model derived here can indeed serve this purpose remains to be seen. While it has been validated for some forced steady and unforced time-dependent flows, the next logical step would be to compare its predictions with experimental observations for forced time-dependent flows. The time-dependent flow in experiment, however, depends rather sensitively on the lateral boundary conditions. Hence, such comparison would require a numerical implementation of the model subject to boundary conditions mimicking those in the experiment. As an alternative, such a comparison could also be performed using a dipolar vortex[30] or a periodic lattice of vortices,[16] although this would require a rather accurate model of the magnetic field.

ACKNOWLEDGMENTS

We thank Daniel Borrero for his valuable suggestions and insights on both experimental and theoretical aspects of the problem. We also thank Phillip First for lending us the Gaussmeter from his laboratory. This work is supported in part by the National Science Foundation under Grant Nos. CBET-0853691, CBET-0900018, and CMMI-1234436.

APPENDIX: ANALYTICAL SOLUTION FOR THE VERTICAL PROFILE $P_0(z)$

Here, we present the analytical expressions for the coefficients C, D, E, F, and u_0 that appear in Eq. (17) for the unidirectional profile $P_0(z)$. Using these, one can compute the values of α, $\bar{\nu}$, and β in the generalized 2D vorticity equation (5). The coefficients have been expressed in terms of quantities s, ΔB, and $\langle B \rangle$ defined in Sec. IV B. Using Eq. (17) and the boundary conditions defined in Eq. (14), we obtain

$$u_0 = s \frac{h_c h_d}{\mu_d} J \langle B \rangle, \tag{A1}$$

$$C = \frac{1}{s} \frac{\mu_d}{\mu_c} \left(\frac{h_c + h_d}{h_c h_d} \right) \left(1 - \frac{1}{2} \frac{h_d}{h_c} \frac{\Delta B}{\langle B \rangle} \right), \tag{A2}$$

$$D = \frac{1}{s} \frac{\mu_d}{\mu_c} \frac{h_d}{h_c} \left[\frac{\mu_c}{\mu_d} \frac{h_c}{h_d} - \frac{h_c}{h_d} - \frac{1}{2} + \left(\frac{1}{4} + \frac{1}{6} \frac{h_d}{h_c} \right) \frac{\Delta B}{\langle B \rangle} \right], \tag{A3}$$

$$E = \frac{1}{h_d s} \quad \text{and} \quad F = 0. \tag{A4}$$

It must be noted that although the value of u_0 computed from (A1) does not correspond to the one experimentally measured for the Kolmogorov-like flow, (A1) captures the scaling of u_0 with experimental parameters.

[1] P. Tabeling, "Two-dimensional turbulence: A physicist approach," Phys. Rep. **362**, 1 (2002).
[2] N. F. Bondarenko, M. Z. Gak, and F. V. Dolzhanskiy, "Laboratory and theoretical models of plane periodic flows," Izv. Akad. Nauk SSSR, Fiz. Atmos. Okeana **15**, 711 (1979).
[3] L. J. Campbell and R. M. Ziff, "Vortex patterns and energies in a rotating superfluid," Phys. Rev. B **20**, 1886 (1979).
[4] J. Sommeria and R. Moreau, "Why, how, and when, MHD turbulence becomes two-dimensional," J. Fluid Mech. **118**, 507 (1982).
[5] A. Pothérat, "Three-dimensionality in quasi-two-dimensional flows: Recirculations and barrel effects," Europhys. Lett. **98**, 64003 (2012).
[6] Y. Couder, "Two-dimensional grid turbulence in a thin liquid film," J. Phys. Lett. **45**, 353 (1984).

[7] T. B. Mitchell, C. F. Driscoll, and K. S. Fine, "Experiments on stability of equilibria of two vortices in a cylindrical trap," Phys. Rev. Lett. **71**, 1371 (1993).
[8] F. V. Dolzhanskii, V. A. Krymov, and D. Y. Manin, "Stability and vortex structures of quasi-two-dimensional shear flows," Sov. Phys. Usp. **33**, 495 (1990).
[9] O. Cardoso, D. Marteau, and P. Tabeling, "Quantitative experimental study of the free decay of quasi-two-dimensional turbulence," Phys. Rev. E **49**, 454 (1994).
[10] M. K. Rivera and R. E. Ecke, "Pair dispersion and doubling time statistics in two-dimensional turbulence," Phys. Rev. Lett. **95**, 194503 (2005).
[11] V. I. Arnold and L. D. Meshalkin, "Seminar led by A. N. Kolmogorov on selected problems of analysis (1958-1959)," Usp. Mat. Nauk **15**, 20 (1960). The English reprint (1961) is available at 10.1016/0021-8928(62)90149-1.
[12] A. M. Obukhov, "Kolmogorov flow and laboratory simulation of it," Russ. Math. Surv. **38**, 113 (1983).
[13] A. Thess, "Instabilities in two-dimensional spatially periodic flows. Part I: Kolmogorov flow," Phys. Fluids A **4**, 1385 (1992).
[14] J. Paret, D. Marteau, O. Paireau, and P. Tabeling, "Are flows electromagnetically forced in thin stratified layers two dimensional?," Phys. Fluids **9**, 3102 (1997).
[15] R. Rivlin, "Run-up and decay of plane poiseuille flow," J. Non-Newtonian Fluid Mech. **14**, 203 (1984).
[16] B. Jüttner, D. Marteau, P. Tabeling, and A. Thess, "Numerical simulations of experiments on quasi-two-dimensional turbulence," Phys. Rev. E **55**, 5479 (1997).
[17] M. P. Satijn, A. W. Cense, R. Verzicco, H. J. H. Clercx, and G. J. F. van Heijst, "Three-dimensional structure and decay properties of vortices in shallow fluid layers," Phys. Fluids **13**, 1932 (2001).
[18] R. A. D. Akkermans, L. P. J. Kamp, H. J. H. Clercx, and G. J. F. Van Heijst, "Intrinsic three-dimensionality in electromagnetically driven shallow flows," Europhys. Lett. **83**, 24001 (2008).
[19] R. A. D. Akkermans, A. R. Cieslik, L. P. J. Kamp, R. R. Trieling, H. J. H. Clercx, and G. J. F. van Heijst, "The three-dimensional structure of an electromagnetically generated dipolar vortex in a shallow fluid layer," Phys. Fluids **20**, 116601 (2008).
[20] R. A. D. Akkermans, L. P. J. Kamp, H. J. H. Clercx, and G. J. F. van Heijst, "Three-dimensional flow in electromagnetically driven shallow two-layer fluids," Phys. Rev. E **82**, 026314 (2010).
[21] D. H. Kelley and N. T. Ouellette, "Onset of three-dimensionality in electromagnetically driven thin-layer flows," Phys. Fluids **23**, 045103 (2011).
[22] D. Marteau, O. Cardoso, and P. Tabeling, "Equilibrium states of two-dimensional turbulence: An experimental study," Phys. Rev. E **51**, 5124 (1995).
[23] M. Nagata, "Three-dimensional traveling-wave solutions in plane couette flow," Phys. Rev. E **55**, 2023 (1997).
[24] R. R. Kerswell, "Recent progress in understanding the transition to turbulence in a pipe," Nonlinearity **18**, R17 (2005).
[25] B. Eckhardt, T. M. Schneider, B. Hof, and J. Westerweel, "Turbulence transition in pipe flow," Annu. Rev. Fluid Mech. **39**, 447 (2007).
[26] J. F. Gibson, J. Halcrow, and P. Cvitanovic, "Equilibrium and travelling-wave solutions of plane Couette flow," J. Fluid Mech. **638**, 243 (2009).
[27] B. Hof, C. W. H. van Doorne, J. Westerweel, F. T. M. Nieuwstadt, H. Faisst, B. Eckhardt, H. Wedin, R. R. Kerswell, and F. Waleffe, "Experimental observation of nonlinear traveling waves in turbulent pipe flow," Science **305**, 1594 (2004).
[28] A. de Lozar, F. Mellibovsky, M. Avila, and B. Hof, "Edge state in pipe flow experiments," Phys. Rev. Lett. **108**, 214502 (2012).
[29] G. J. Chandler and R. R. Kerswell, "Invariant recurrent solutions embedded in a turbulent two-dimensional Kolmogorov flow," J. Fluid Mech. **722**, 554 (2013).
[30] A. Figueroa, F. Demiaux, S. Cuevas, and E. Ramos, "Electrically driven vortices in a weak dipolar magnetic field in a shallow electrolytic layer," J. Fluid Mech. **641**, 245 (2009).
[31] A. Thess, "Instabilities in two-dimensional spatially periodic flows. Part II: Square eddy lattice," Phys. Fluids A **4**, 1396 (1992).
[32] A. Thess, "Instabilities in two-dimensional spatially periodic flows. Part III: Inviscid triangular lattice," Phys. Fluids A **5**, 335 (1993).
[33] V. Dovzhenko, A. Obukhov, and V. Ponomarev, "Generation of vortices in an axisymmetric shear flow," Fluid Dyn. **16**, 510 (1981).
[34] F. V. Dolzhanskii, V. A. Krymov, and D. Y. Manin, "An advanced experimental investigation of quasi-two-dimensional shear flow," J. Fluid Mech. **241**, 705 (1992).
[35] G. Boffetta, A. Cenedese, S. Espa, and S. Musacchio, "Effects of friction on 2d turbulence: An experimental study of the direct cascade," Europhys. Lett. **71**, 590 (2005).